

A MODIFIED SCHWARZ-CHRISTOFFEL TRANSFORMATION FOR ELONGATED REGIONS*

LOUIS H. HOWELL† AND LLOYD N. TREFETHEN‡

Dedicated to the memory of Peter Henrici.

Abstract. The numerical computation of a conformal map from a disk or a half plane onto an elongated region is frequently difficult, or impossible, because of the so-called crowding phenomenon. This paper shows that this problem can often be avoided by using another elongated region, an infinite strip, as the standard domain. A transformation similar to the Schwarz-Christoffel formula maps this strip onto an arbitrary polygonal channel, and a slightly modified transformation maps an elongated rectangle onto an arbitrary closed polygon. By using robust and efficient software for numerical integration and solution of the parameter problem, high-accuracy maps of distorted regions with aspect ratios as high as thousands to one are constructed. The modified mapping method has natural applications in fluid mechanics and electrical engineering.

Key words. Schwarz-Christoffel transformation, conformal mapping, elliptic functions, crowding, grid generation

AMS(MOS) subject classifications. 30C30, 30C20

1. Introduction. The Schwarz-Christoffel transformation

$$(1.1) \quad f(z) = A \int^z \prod_{j=1}^n (z' - z_j)^{\gamma_j} dz' + B$$

provides an explicit representation of any conformal map of the unit disk or the upper half plane onto any simply connected polygonal region, with or without corners at infinity. There are two well-known computational problems associated with the use of this formula for computing such maps numerically. First, the integral cannot be evaluated analytically except in special cases, and must be approximated by some numerical procedure. Second, while the parameters γ_j are determined by the angles at the vertices w_j of the polygon, the corresponding “prevertices” $z_j = f^{-1}(w_j)$ cannot be determined, in general, a priori and must be obtained iteratively via the solution of a system of nonlinear equations. SCPACK, a robust Fortran package for solving these problems, was provided a few years ago by Trefethen [28], [29] and has been widely used for a variety of applications.¹ Other successful implementations of the Schwarz-Christoffel formula include those of Reppe [26], Davis [3], Floryan [10], Hoekstra [19], and Dias [5].

Standard Schwarz-Christoffel programs fail, however, on some seemingly very simple polygons. They cannot, for example, map a rectangle with an aspect ratio of only 20 to 1, or most other regions with a similar degree of elongation. The reason for this is an intrinsic property of conformal maps that sometimes goes by the name of the “crowding phenomenon” in the literature of numerical conformal mapping (see [7], [14], [18], [21], [31]). Whenever a disk or half plane is mapped to an elongated

* Received by the editors July 5, 1988; accepted for publication (in revised form) June 16, 1989. This work was supported by U.S. Air Force grant AFOSR-87-0102.

† Lawrence Livermore Laboratory, L-419, Livermore, California 94550.

‡ Department of Mathematics, Massachusetts Institute of Technology, Cambridge, Massachusetts 02139.

¹ Available by electronic mail from the “Netlib” facility [6].

region, some of the prevertices are located exponentially close together. For aspect ratios beyond 10 or 20 some groups of prevertices are likely to merge together in finite precision arithmetic, making the evaluation of (1.1) effectively impossible.

Fortunately, many of the distorted regions that come up in applications are highly elongated in only one direction. Indeed, the goal in such problems is often to map the region onto a channel or rectangle for purposes of grid generation or to obtain an exact or simplified solution; a disk or half plane is introduced only as an intermediate step. The purpose of this paper is to show that in such cases, the problem of crowding can be largely eliminated by dispensing with the intermediate domain and mapping directly from an infinite strip, which can be easily transformed to a rectangle if desired. In the language of numerical analysis, constructing the conformal map from a strip to an elongated polygon is often a well-conditioned problem, but conventional algorithms for it are unstable because they depend upon the solution of an ill-conditioned subproblem. Our algorithm is stable because it avoids the subproblem.

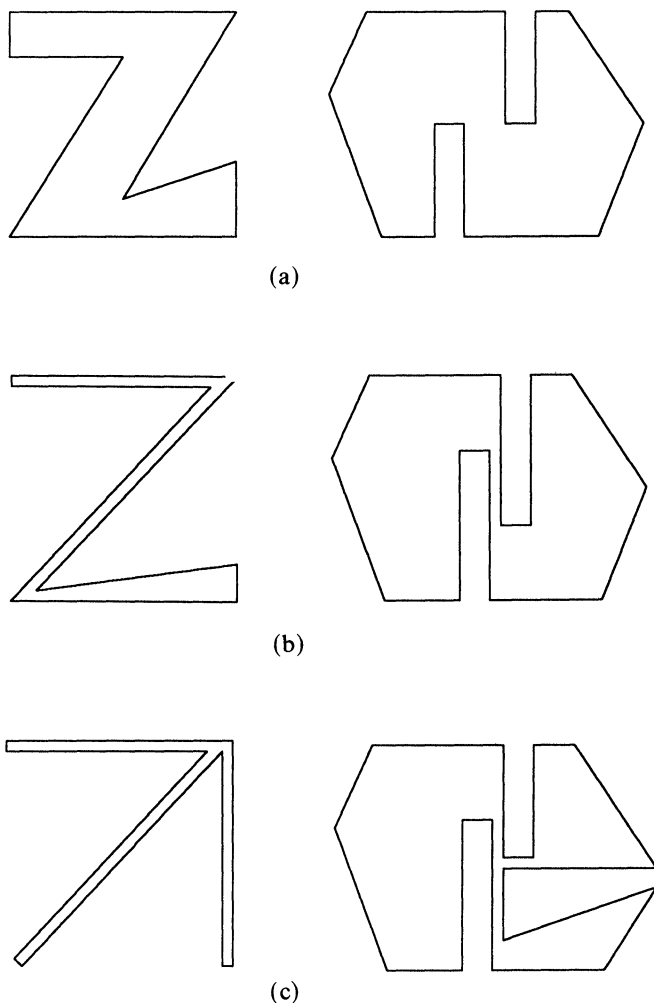


FIG. 1. (a) Polygons that can be mapped by the standard Schwarz-Christoffel transformation; (b) polygons that can be mapped by the strip transformation; and (c) polygons that cannot be mapped by either method.

The capabilities described in this paper are summarized in Fig. 1(a)-1(c). Many polygons, those without extreme elongation in any direction, can be mapped by the standard Schwarz-Christoffel methods embodied in SCPACK (Fig. 1(a)). Polygons that are highly elongated in one direction (as well as those that are not elongated) can be mapped by the modified Schwarz-Christoffel methods described here (Fig. 1(b)). For polygons elongated in several directions, different methods will be required (Fig. 1(c)).

The basis of our algorithm is a formula similar to (1.1) for mapping an infinite strip onto an arbitrary polygonal channel (§ 3), and a variation of this formula for mapping a rectangle onto a closed polygon (§ 6). These formulas are not essentially new; the first one dates back at least to Woods [33] and has been used previously by Davis [3], Sridhar and Davis [27], and Floryan [9], [10] for generating computational grids for internal flow problems. The present work differs, however, in emphasizing the crowding phenomenon and in considering the mapping of rectangles to closed polygons as well as other variations. Although it is impossible to be certain in the absence of a direct comparison of computer programs, we believe that our solution method is robust enough to permit the mapping of more complicated regions than those attempted previously. Possible applications of this work include the solution of two-dimensional potential flow problems, the construction of computational grids, the calculation of circuit properties in integrated circuit design [30], and the application of boundary conditions in vortex-method simulations of high Reynolds number flow [15]. For the last example, boundary conditions in vortex calculations, it would be natural to combine the conformal map to an infinite strip discussed here with L. Greengard's recent algorithm for fast calculation of vortex interactions in such a strip [17].

A general method for deriving certain types of Schwarz-Christoffel variations, including the strip formula used here, is presented in [11]. An informal survey of such variations and of applications of Schwarz-Christoffel maps can be found in [32].

Although this paper considers only Schwarz-Christoffel maps, similar ideas might prove useful for more general conformal mapping problems. For example, it would be natural to investigate variants of the Theodorsen, Wegmann, or Hübner methods for mapping an infinite strip onto an elongated region with a curved boundary (see [18], [31]).

2. The crowding problem. The phenomenon of crowding began to be widely recognized as an obstacle to successful numerical conformal mapping around 1980; the term "crowding" itself is due to Menikoff and Zemach [21]. To illustrate this phenomenon, we will examine a simple example that can be treated analytically. The Jacobian elliptic function $\operatorname{sn}(z|m)$ maps the rectangle with corners $-K$, K , $K + iK'$, and $-K + iK'$ to the upper half plane, with the images of the corners being ± 1 and $\pm m^{-1/2}$ (Fig. 2). The constants K and K' are complete elliptic integrals with parameters m and $m_1 = 1 - m$, respectively, so only one of K , K' , and m can be specified independently. A summary of the properties of elliptic functions and elliptic integrals, including all of the material used in this paper, can be found in [1].

The conformal modulus μ of the rectangle is $K'/2K$, and $m^{1/2}$ can be used as a measure of the crowding effect since it is the ratio of the smallest to the largest length scales in the upper half plane. When μ is large the following asymptotic relationships hold:

$$(2.1) \quad K \sim \frac{\pi}{2}, \quad K' \sim \pi\mu, \quad m^{1/2} \sim 4 e^{-\pi\mu}.$$

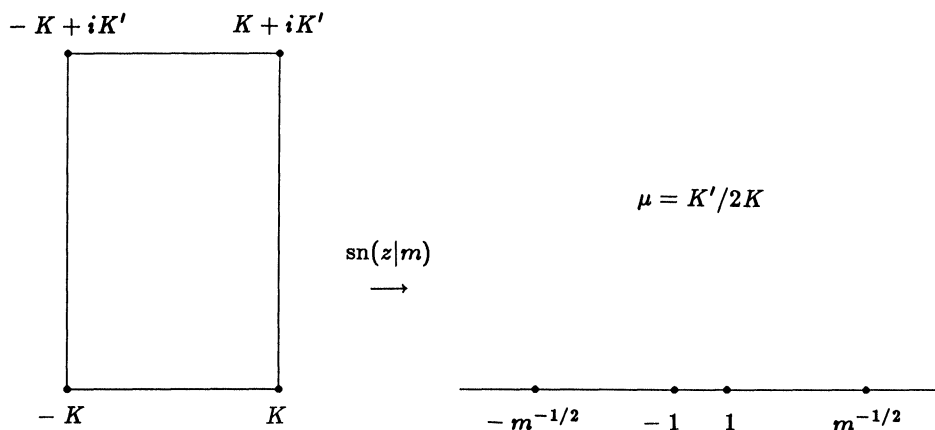


FIG. 2. Conformal map from a rectangle to the upper half plane.

Thus for a modulus of only $\mu = 10$, for instance, the important length scales in the upper half plane vary by factors on the order of 10^{13} .

It might seem that these difficulties are surmountable, since in this example all of the crowding occurs near the origin. In floating-point arithmetic the four numbers ± 1 and $\pm m^{-1/2}$ can all be represented to full accuracy, even though the first two may be many orders of magnitude smaller than the last two. There are several reasons, though, why this is an unsatisfactory approach. First, many computers have a range of permissible exponents too restricted to deal with conformal moduli greater than 25 or 50. Second, such a highly distorted mapping would be useless in many applications. Finally, the direct numerical evaluation of the integral (1.1) in such a situation would require a highly specialized quadrature algorithm. A natural first step in such an algorithm would be to change the variable of integration to $\log(z')$, which is in fact equivalent to using the strip transformation.

Figure 3 shows the crowding effect in the conformal map from the unit disk to a mildly elongated region. The four rectangles have moduli 1, 2, 3, and 4, and the internal lines shown are the images of radii to the four prevertices and of equally spaced concentric circles in the unit disk. Due to the conformal nature of each mapping, the innermost circle in each plot is nearly similar to the original disk, so in effect these figures show both the domain and range of each transformation. In particular, we can see the relative positions of the prevertices, and their angular separations are listed in the figure. In the bottom plot, with a conformal modulus of only 4, each of the two pairs of prevertices appears to the eye as a single point. For moduli three or four times larger than this the pairs fuse together in floating-point arithmetic, and the computation by standard methods becomes impossible.

It should be emphasized that crowding occurs when any portion of a domain is elongated. If the rectangles in Fig. 3, for instance, were all extensions of a larger region to the left, then each one would still experience a crowding effect like that shown in the figure. A strongly acute outward-pointing corner can cause a similar problem (for a mild example, see the barb on the arrow in Fig. 10(a)). The methods considered in this paper do not eliminate these secondary crowding effects, which degrade the local accuracy of the mapping and may in extreme cases cause the solution method to fail. In many cases, however, high accuracy can still be obtained in the remainder of the domain.

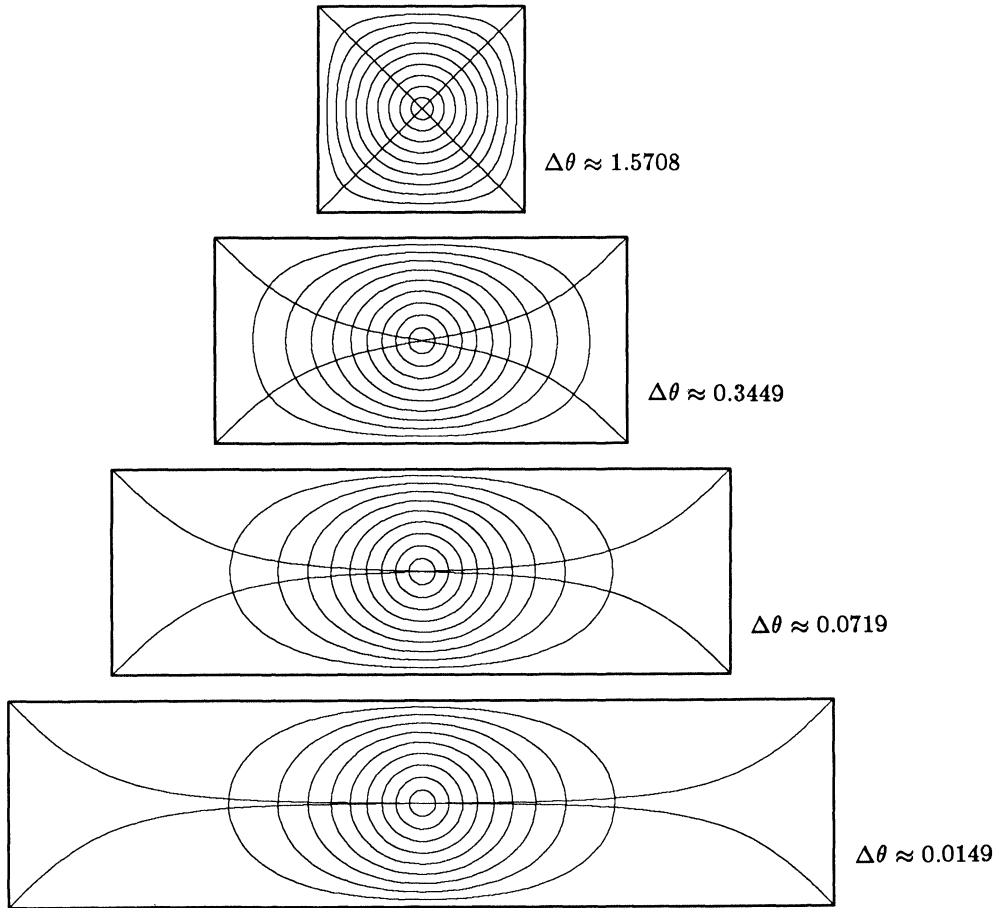
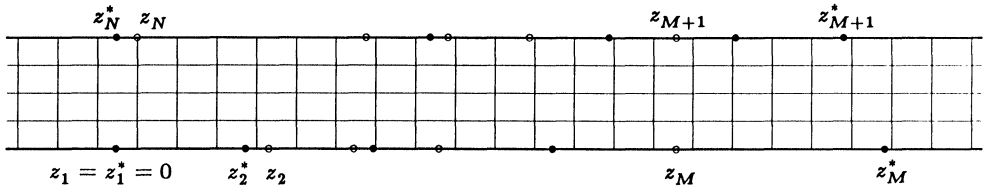


FIG. 3. Conformal maps of the unit disk onto four rectangles.

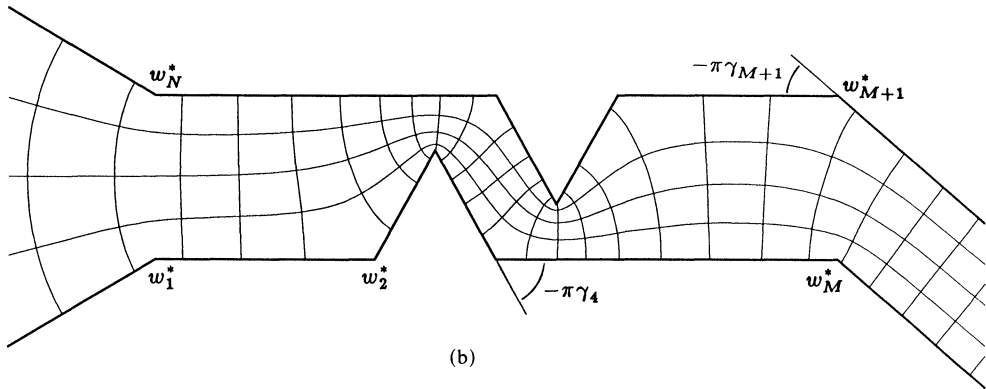
3. The strip transformation. In this section we derive a formula for the conformal map of an infinite strip onto a polygon (3.5); essentially the same formula has been derived earlier (in different ways) by Davis [3] and by Floryan and Zemach [11]. We shall not provide a proof that any conformal map of an infinite strip to a polygon can be represented in this way, but it is true, and a proof can be readily obtained from the standard Schwarz–Christoffel theorem by means of the transformation $e^{\pi z}$ from a strip to a half plane [3].

Figure 4(a)–4(c) defines the geometry of our strip mapping problem: We want to find a conformal map f^* from an infinite strip of width 1 to an infinite polygonal channel P^* . Our notation is that z_j^* and $w_j^* = f^*(z_j^*)$ denote prevertices and vertices for this desired conformal map, while z_j and $w_j = f(z_j)$ correspond to the conformal map onto a polygon $P \approx P^*$ obtained during the course of the numerical solution. The prevertices z_j lie in counterclockwise order around the strip, starting with z_1 on the lower left, proceeding through z_M on the lower right, and ending with z_N on the upper left. The corresponding vertices of the image polygon are denoted by w_j , and the turning angle at w_j is $-\pi\gamma_j$.

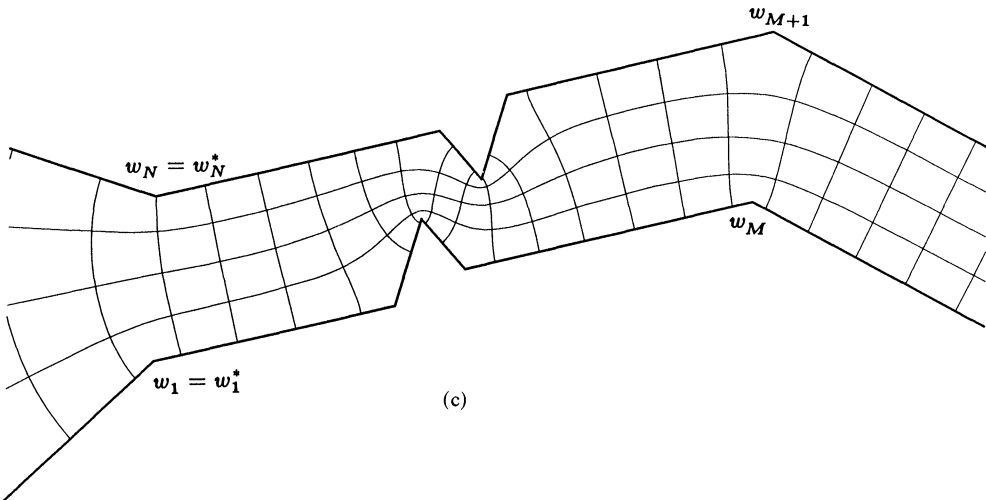
Here is the fundamental idea behind the Schwarz–Christoffel map (1.1): the derivative $f'(z)$ has piecewise constant argument on the real axis, which jumps at each prevertex z_j by $-\pi\gamma_j$. To devise a transformation that maps an infinite strip onto an



(a)



(b)



(c)

FIG. 4. (a) *Prevertices on the strip*: solid dots show the correct values z_j^* , and open circles show an incorrect set of values z_j ; (b) *target polygon P^** defined by vertices w_j^* ; (c) *polygon P* defined by incorrect vertices w_j .

arbitrary polygon, we can utilize the same idea. Specifically, let us derive a function of the form

$$(3.1) \quad f(z) = A \int^z \prod_{j=1}^n f_j(z') dz' + B,$$

where each factor f_j maps the strip as shown in Fig. 5. The effect of each of these factors is to introduce a corner into one side of the strip while leaving the other side

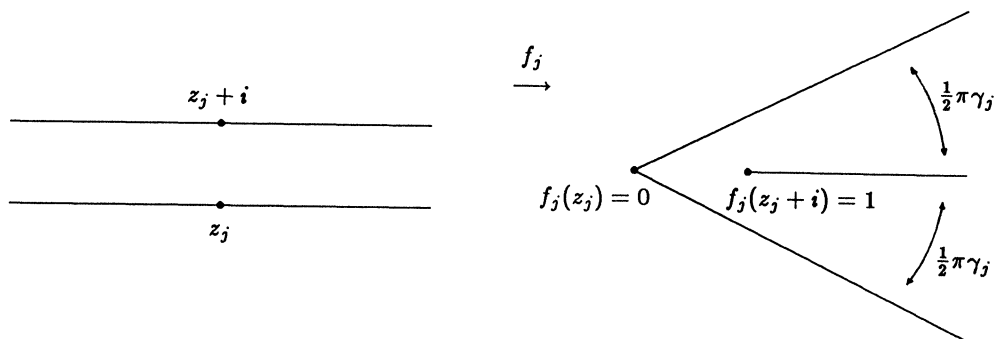


FIG. 5. A single factor f_j , shown for $\gamma_j > 0$.

a straight line. The product of several such factors will introduce all of the necessary corners.

The appropriate factors f_j that meet these specifications are very similar to those used in the usual Schwarz-Christoffel formula: For z_j on the lower side of the strip,

$$(3.2) \quad f_j(z) = \left\{ -i \sinh \left[\frac{\pi}{2} (z - z_j) \right] \right\}^{\gamma_j}, \quad 1 \leq j \leq M,$$

and for z_j on the upper side,

$$(3.3) \quad f_j(z) = \left\{ -i \sinh \left[-\frac{\pi}{2} (z - z_j) \right] \right\}^{\gamma_j}, \quad M + 1 \leq j \leq N.$$

In each of these factors the effect of the sinh function is to fold the opposite side of the strip from z_j onto part of the imaginary axis, while the side containing z_j is sent to the real axis. Each section of the boundary is therefore mapped to a line of constant argument, and these remain lines of constant argument after the function is raised to the power γ_j . This property is necessary if the sides of the target domain are to be straight lines. The factors of $-i$ in these equations are mathematically unnecessary, since they can be absorbed into the complex constant A . We have included them, however, to direct the branch cuts of the f_j away from the strip. (Conventionally, and in Fortran, these branch cuts are located on the negative real axis.)

The functions f_j of (3.2) and (3.3) introduce the required angles at the vertices on both sides of the channel, but they always produce equal divergence angles at $\pm\infty$. If we let θ_- and θ_+ be the desired divergence angles at $-\infty$ and $+\infty$, respectively, then the additional factor

$$(3.4) \quad f_0(z) = \exp\left[\frac{1}{2}(\theta_+ - \theta_-)z\right]$$

provides the necessary adjustment. The full strip transformation is thus given by

$$(3.5) \quad f(z) = A \int^z \prod_{j=0}^n f_j(z') dz' + B,$$

where the individual functions f_j are defined by (3.1)–(3.4).

4. Solving the parameter problem. How can the prevertices z_j^* be efficiently determined? If prevertices z_j are placed on the correct sides of the strip and in the proper order, but otherwise distributed at random, then the image polygon will in general have the correct angles but incorrect side lengths (Fig. 4). Some kind of iteration must be carried out to find the values z_j^* so that the side lengths come out correct.

As usual in conformal mapping, three real parameters must be specified in order to make f unique. In mapping an infinite strip to an infinite channel, it is natural that the ends of the strip should map to the ends of the channel, so two of these are determined immediately. We have specified the third parameter by fixing z_1^* at the origin; the remaining $N - 1$ prevertices z_2^*, \dots, z_N^* are now the unknowns to be determined iteratively. If the constants A and B in (3.5) are used to fix the positions of w_1 and w_N , then there are correspondingly $N - 1$ real geometric conditions— $N - 2$ side lengths and one angle—needed to completely specify the shape of the channel.

4.1. Solution via side-length iteration. One popular method for determining the prevertex positions is a simple iterative scheme used by Davis [3] for the standard Schwarz-Christoffel formula. The idea is to make an initial guess for the z_j and then improve it by assuming that the length of each side of the image polygon is roughly proportional to the length of the corresponding interval on the real axis. Thus each interval between prevertices is adjusted according to the formula

$$(4.1) \quad (z_{j+1} - z_j)_{\text{new}} := (z_{j+1} - z_j) \cdot \frac{|w_{j+1}^* - w_j^*|}{|w_{j+1} - w_j|}.$$

By iterating this procedure it is hoped that the correct solution can be obtained to the desired accuracy. This method has also been used by Floryan [9], [10] and Sridhar and Davis [27], and is quite dependable for many problems. We believe it is not the best choice for a general algorithm, however, for the following reasons:

- When used with the strip transformation, the method gives no information about the position of z_N^* , the leftmost prevertex on the top side of the strip. Sridhar avoids this problem by restricting attention to channels where symmetry implies $z_N^* = i$. Floryan uses a double iteration for the asymmetric case—a one-dimensional secant iteration determines a value for z_N at each step of the global iteration (4.1).
- The proportionality assumption can be violated by difficult problems in at least two different ways. First, it assumes that only the preimages at the endpoints of an interval have a major effect on the length of the corresponding side, and this condition is violated when crowding occurs. Second, if the two singularities at the endpoints are strong, i.e., the interior angles are acute, then the length of the side may actually decrease as the prevertex separation increases. Even with the standard Schwarz-Christoffel formula there are geometries for which (4.1) fails to converge, and with the strip transformation we have the added problem that singularities on the opposite side of the strip may also strongly influence an interval.

Despite these difficulties, the iteration (4.1) often converges within at most a few tens of iterations, particularly on relatively straightforward problems like those shown in Figs. 4 and 6. On a region like that shown in Fig. 8, however, it diverges even when started very near the solution. (Figure 8 actually shows an example of a map from a rectangle to a closed polygon. The same geometry can be treated as a channel, though, if the right angles at the ends are replaced by straight angles. The prevertex z_N is so far “upstream” in this case that it does not cause significant problems; the main area of difficulty for (4.1) is at the other end of the figure. On this example we have used the high-accuracy adaptive quadrature methods described in § 5—though somewhat inefficient, these routines give quite reliable error bounds, so the failure cannot simply be caused by an inaccurate quadrature algorithm.)

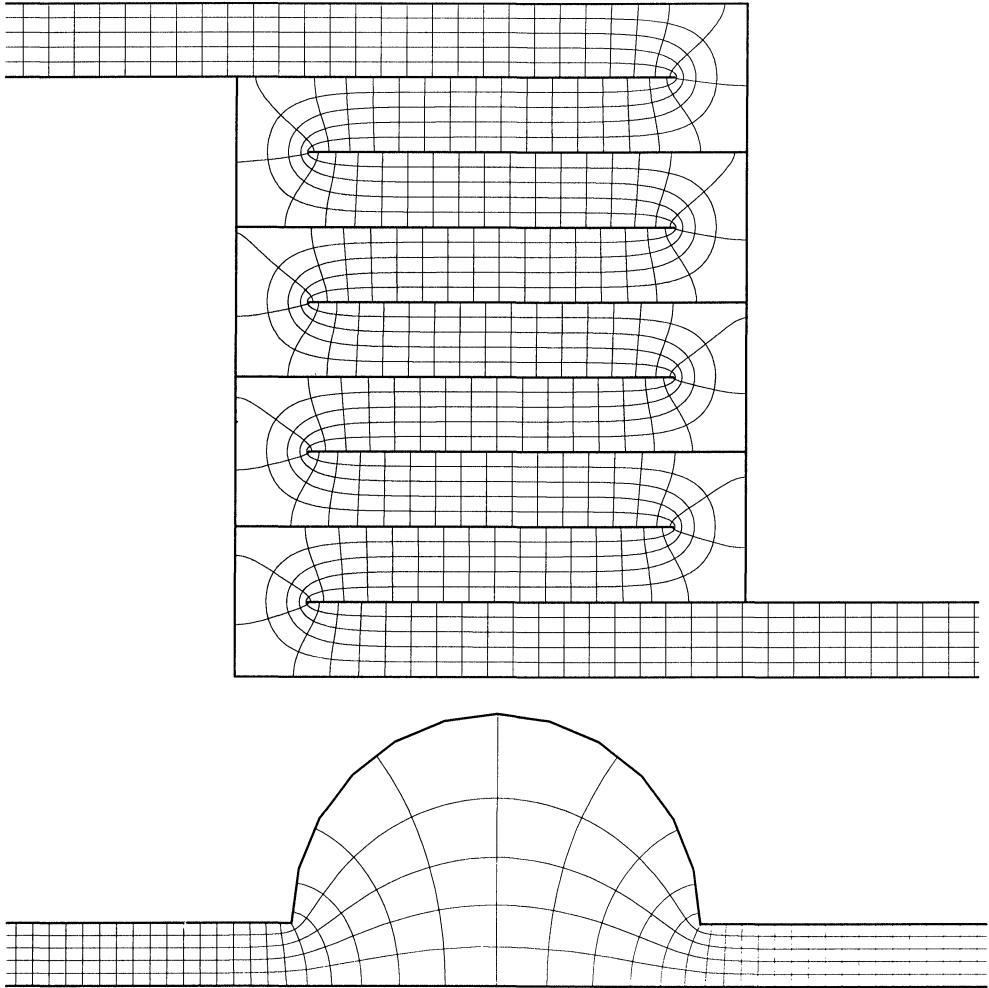


FIG. 6. Two channels with large N .

Further examples supporting these claims will be presented in a future paper.

- The convergence is only linear, which may be a disadvantage for high-accuracy computations.
- Many Schwarz-Christoffel problems that arise in applications come with additional conditions to be satisfied. For example, the conformal modulus μ might be specified in advance and one of the side lengths left unspecified. In such situations one has a “generalized parameter problem” to solve [30], which may not be an easy matter if one is using an iteration like (4.1) that is dependent on geometric insight.

4.2. Solution via secant iteration. In our own calculations we have instead viewed the parameter problem as a general system of nonlinear equations $\mathbf{F}(\mathbf{x}^*) = \mathbf{0}$ to be solved numerically; this is an old idea. The normalization described above fixes z_1 , so an obvious choice for the $N - 1$ independent variables might be $\operatorname{Re}(z_2), \dots, \operatorname{Re}(z_N)$. This choice leads to a constrained system, however, since the prevertices on each side

of the strip must appear in the proper order. To remove the constraints, we have used a change of variables similar to the one in SCPACK:

$$(4.2) \quad x_j = \begin{cases} \operatorname{Re}(z_N), & j = 1, \\ \log(z_j - z_{j-1}), & 2 \leq j \leq M, \\ \log(z_j - z_{j+1}), & M + 1 \leq j \leq N - 1. \end{cases}$$

As for the dependent variables, we first compute the positions of w_1, \dots, w_N by integrating (3.5) and using the constants A and B to fix w_1 and w_N at their correct positions. The $N - 1$ functions to be set to zero are then given by

$$(4.3) \quad F_j = \begin{cases} \operatorname{Im} \left[\log \left(\frac{w_2 - w_1}{w_2^* - w_1^*} \right) \right], & j = 1, \\ \operatorname{Re} \left[\log \left(\frac{w_j - w_{j-1}}{w_j^* - w_{j-1}^*} \right) \right], & 2 \leq j \leq M, \\ \operatorname{Re} \left[\log \left(\frac{w_j - w_{j+1}}{w_j^* - w_{j+1}^*} \right) \right], & M + 1 \leq j \leq N - 1. \end{cases}$$

F_1 is an angle, and each of the other F_j involves the logarithm of a side length. The use of logarithms improves the scaling of the problem when some sides are much longer than others, as often occurs with elongated regions.

We have experimented with three nonlinear equations packages for solving this problem: Powell's subroutine NS01A [25], the Minpack routine HYBRD [22], and an implementation of Schnabel's pseudocode from Dennis and Schnabel [4]. All three are based on a hybrid (dogleg) quasi-Newton algorithm with secant updates. On average we obtained slightly better results with HYBRD, and in addition one of our test problems caused Powell's code to fail. (This difficulty was apparently due to an overly strict stopping criterion rather than a fundamental failure of the algorithm.) Some of our test problems were quite difficult, involving extremely distorted polygons like those shown later in the paper; such problems sometimes required several hundred evaluations of the functions (4.3). The only cases where either HYBRD or Schnabel's code failed eventually to find a solution involved severe crowding in regions that were elongated in more than one direction, as in Fig. 1(c). Though for individual problems there were sometimes wide variations in the number of iterations required by the different routines, all three gave fairly similar performance when averaged over a number of different cases.

Dias [5] and Bjørstad and Grosse [2] have used other nonlinear equations packages for Schwarz-Christoffel problems, with similar results.

In the context of this section, Davis' algorithm (4.1) can be thought of as an approximate Newton iteration in which an approximate Jacobian is estimated from geometrical considerations; our second observation in § 4.1 above amounts to the statement that sometimes this approximation may fail to yield a descent direction.

The secant algorithms converge superlinearly once they are near the solution (see [4]), but for difficult problems they may take a long time to get near it. Convergence times seem to be nearly independent of the starting point, a clear indication that we do not have a good algorithm for picking starting points. To examine the typical convergence rate as a function of N , at least two different types of problems should be considered, as shown in Fig. 6. In the first example the geometry becomes progressively more complicated as N increases, while in the second the geometry is roughly constant, and increasing N merely improves the resolution of the curved part of the boundary. (There are better ways to approximate curved boundaries; see [9] and [27].)

In practice, we find that for problems of the first kind the number of iterations required is roughly $O(N)$, whereas for problems of the second kind it is closer to $O(1)$. Since each evaluation of (4.3) requires $O(N^2)$ operations, and the evaluation of the initial Jacobian matrix by finite differences requires N evaluations, the total work required to solve the parameter problem is at least $O(N^3)$ in both cases.² For N less than about 50 the Jacobian evaluation is not the dominant factor in the calculation, however, so problems with simple geometries typically display behavior closer to $O(N^2)$.

5. Evaluating Schwarz–Christoffel integrals. The second numerical problem is the evaluation of (3.5). This cannot be done analytically, and is somewhat difficult numerically because of the singularity in the integrand at each prevertex z_j . A robust integration scheme must be able to deal efficiently not only with the endpoint singularities that occur when one of the limits of integration is a prevertex, but also with the nearly singular situation where a prevertex is very close to the interval of integration. The latter case is important when there is significant crowding, and also when a nearby singularity lies on the opposite side of the strip from the interval of interest. Removing every possible singularity analytically would not be worth the trouble, but neither would refining the mesh over the entire interval just to deal with a few difficult segments. In SCPACK, Trefethen [28] used a compound Gauss–Jacobi quadrature algorithm with considerable success. This method outperforms every alternative we have tried, but since it lacks an internal error check, we have sometimes found it helpful to supplement it with more general adaptive quadrature schemes. The first use of general adaptive quadrature routines for Schwarz–Christoffel integrals appears to be that of Dias [5] as late as 1986.

Singularities at the endpoints themselves are more of a nuisance than a problem since they can be directly accounted for by the quadrature algorithm. The first question is whether we have to integrate them at all. In their program for solving the Schwarzian differential equation for circular arc polygons, Bjørstad and Grosse [2] avoid singularities by integrating to the midpoint of each interval instead of to each prevertex. Corner positions are then found by calculating where sides intersect. However, this approach can run into trouble for difficult regions, particularly when the program is far from a solution to the parameter problem. We have seen examples where the initial guess for the prevertices yielded an image polygon with some side lengths incorrect by factors exceeding 10^{16} . In such examples, adjacent corners may become indistinguishable even in double precision. By contrast, integrating (3.5) directly from one corner to the next permits each side length to be determined individually without cancellation problems.

5.1. Adaptive quadrature. Given that we choose to integrate up to singularities, there are a number of methods to choose from. We can either use a quadrature rule that explicitly takes the singularity into account, such as a Gauss–Jacobi or Clenshaw–Curtis formula, or we can attempt to remove the singularity analytically so that a standard quadrature rule can be used. QUADPACK [24] includes routines that take the explicit approach. The most effective of these for our Schwarz–Christoffel problem is QAWS, an adaptive quadrature subroutine that uses a Gauss–Kronrod formula in the interior and a Clenshaw–Curtis formula near the singularities. All of the adaptive QUADPACK routines, however, seem to be written with the assumption that typical integrals will be very difficult. They use very high-order rules and require a large

² The linear algebra required by the secant algorithm can be held to $O(N^2)$ per iteration by using secant updates (see [4]), and is typically negligible compared with the cost of evaluation (4.3).

number of integrand evaluations—50 for QAWS—even when no adaptive refinement is necessary. Since many of the integrals involved in any Schwarz–Christoffel problem are not at all difficult, this expense makes QUADPACK less competitive unless high accuracy is required.

When only moderate accuracy (fewer than eight decimal places) is required in the evaluation of (3.5), we have obtained better performance by using singularity removal along with QUANC8, a simple adaptive routine described in [13]. QUANC8, based on the 8-panel Newton–Cotes formula, is more efficient than the routines in QUADPACK when many of the integrals are well behaved. For solving the parameter problem the 8-panel rule seems to be a good compromise between accuracy and speed, although modified versions of QUANC8 based on lower-order formulas are better for applications involving shorter intervals of integration, e.g., graphics. The key point is that for efficiency an integrator must solve simple problems quickly, whereas for robustness it must include an internal error check and must be able to adaptively refine its mesh if necessary.

5.2. Compound Gauss–Jacobi quadrature. The problem with the adaptive integrators described above is that they do not use all of the available information. Their algorithmic decisions are based solely on the observed behavior of the integrand, whereas in Schwarz–Christoffel problems we know the precise position and strength of every singularity before integration begins. Compound Gauss–Jacobi quadrature is a compromise between fixed-rule algorithms, which are unsatisfactory due to nearby singularities, and fully adaptive algorithms, which are extremely dependable but relatively slow. The idea is to use a Gauss–Jacobi formula on each interval that ends at a singularity and an ordinary Gauss formula on all other intervals, with the rather arbitrary requirement that no outside singularity may lie closer to any interval than half the length of that interval [28]. In our program we implement this by splitting any interval that is too close to a singularity in half recursively, repeating as necessary until every interval of integration is short enough to be acceptable. The nodes and weights for the Gauss–Jacobi quadrature rules are calculated using the routine GAUSSQ by Golub and Welsch [16]; we have found experimentally that the number of accurate decimal places in the solution is approximately the same as the number of nodes used on each interval. The primary drawback of the method is that this is entirely an empirical bound.

In our computations the compound Gauss–Jacobi method has outperformed adaptive rules by a factor of at least 2. There are several ways in which it could be improved—for example, by taking the strengths as well as the positions of outside singularities into account. Perhaps theorems could be developed to establish that a suitably defined compound Gauss–Jacobi algorithm is guaranteed to be successful; in the meantime, a virtually foolproof error bound can be obtained if desired by switching to a high-accuracy adaptive integrator at the end of the solution of the parameter problem. On the other hand, since graphics do not require high accuracy, we have also found it efficient to switch to a low-accuracy adaptive method, based on Simpson’s rule, for plotting the final map. Other low-accuracy integration formulas suitable for Schwarz–Christoffel mapping are described in a recent paper by Floryan and Zemach [12].

5.3. Singularity removal. When using a quadrature package that does not explicitly take singularities into account, it is necessary to remove endpoint singularities from the integrand analytically. There are two main methods for removing singularities, and we have found it difficult to pick one as a favorite. If for simplicity we place the

singularity at 0, the problem is to integrate a function $f(x) = x^\gamma g(x)$, where g is analytic at 0 and $\gamma > -1$, on an interval $(0, X)$. Expanding $f(x)$ in a power series about 0, we obtain

$$(5.1) \quad f(x) = x^\gamma g(0) + x^{\gamma+1} g'(0) + \frac{1}{2} x^{\gamma+2} g''(0) + O(x^{\gamma+3}).$$

The first method for removing the singularity is simply to subtract off the leading terms of (5.1), which can be integrated analytically, and to use a numerical integrator only on the relatively well-behaved remainder. With just the first term removed the remainder may have an infinite slope at 0, which is still enough to cause serious trouble for integrators that assume polynomial behavior. With the first and second terms removed, though, most polynomial integrators perform quite well near the singularity. The use of this two-term subtraction for Schwarz–Christoffel problems dates back at least to Kantorovich and Krylov [20].

The second standard method is to find a change of variables $x = t^\alpha$ such that the integrand is well behaved when expressed in terms of t . In general, we want to choose α so that for $t \approx 0$, $f[x(t)] d[x(t)]$ will behave like $t^\beta dt$ for some small nonnegative integer β . A little algebra gives $\alpha = (\beta + 1)/(\gamma + 1)$. The new integrand is then $\alpha t^{\alpha-1} f(t^\alpha)$, which indeed has the expected leading-order behavior near $x = 0$. Dias [5] used this method with $\beta = 0$, which works quite well for $-1 < \gamma \leq 0$. However, we have found that polynomial integrators still have trouble with the transformed integrand when $\gamma > 0$. To see why this happens, let us expand f again and look at what the change of variables does to the higher-order terms:

$$(5.2) \quad f(x) = x^\gamma (g_0 + g_1 x + g_2 x^2 + O(x^3)),$$

$$(5.3) \quad \begin{aligned} f(t^{(\beta+1)/(\gamma+1)}) &= g_0 t^{\gamma(\beta+1)/(\gamma+1)} + g_1 t^{(\gamma+1)(\beta+1)/(\gamma+1)} \\ &\quad + g_2 t^{(\gamma+2)(\beta+1)/(\gamma+1)} + O(t^{(\gamma+3)(\beta+1)/(\gamma+1)}), \end{aligned}$$

$$(5.4) \quad \begin{aligned} t^{(\beta-\gamma)/(\gamma+1)} f(t^{(\beta+1)/(\gamma+1)}) &= g_0 t^\beta + g_1 t^{\beta+(\beta+1)/(\gamma+1)} \\ &\quad + g_2 t^{\beta+2(\beta+1)/(\gamma+1)} + O(t^{\beta+3(\beta+1)/(\gamma+1)}). \end{aligned}$$

Note that the g_1 term can have an infinite-slope singularity when $\beta = 0$ and $\gamma > 0$. The obvious solution to the problem is to use a larger β , but there is a trade-off involved since the resulting large value of α makes the integrand evaluation points cluster near the singularity, so that the adaptive integrator must work harder at the other end of the interval. We have found empirically that using $\beta = 0$ for $\gamma < -0.35$, $\beta = 1$ otherwise, tends to give the best results, which are slightly better than those obtained using the method of Kantorovich and Krylov.

6. Mapping rectangles to closed polygons. When the target domain is a closed polygon rather than an infinite channel, it is often appropriate to take an elongated rectangle as the standard region rather than an infinite strip.³ The aspect ratio of the rectangle will be equal to the conformal modulus (\approx electrical resistance) of the original polygon with its four distinguished vertices. We calculate this conformal map by mapping first from the rectangle to the strip by means of an elliptic function, then from the strip to the polygon by the strip transformation.

The function $s(z) = (1/\pi) \log \operatorname{sn}(z|m)$ maps a rectangle onto a strip of width 1, sending the corners $-K$, K , $K + iK'$, and $-K + iK'$ of the rectangle to the points i , 0 , L , and $L + i$, respectively, where K , K' , and L are all functions of m (Fig. 7). It seems reasonable to require each corner of the rectangle to map to a vertex of the polygon,

³ For other approaches to conformal mapping onto rectangles, see [14] and [23].

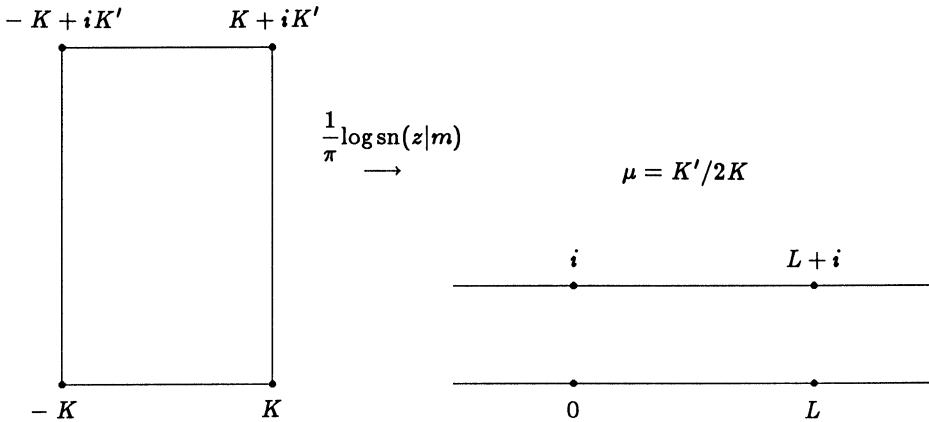


FIG. 7. Conformal map from a rectangle to a strip.

and in many applications this is called for since the conformal modulus is required. However, the formulation of the parameter problem that we used in § 4 would not permit this since, in general, no two prevertices have the same real part. We can avoid this difficulty, though, since for a closed polygon we no longer need to specify the images of the ends of the strip. The two extra degrees of freedom thus obtained can be used instead to fix z_N^* at i and require that the two rightmost prevertices have the same real part. Solving the parameter problem with these restrictions thus gives us an appropriate value for L , from which m , K , and K' can be calculated using the known properties of elliptic functions.

In formulating the parameter problem for this version of the strip transformation, we again use the constants A and B in (3.5) to send w_1 and w_N to their correct positions. A suitable set of unconstrained independent variables, corresponding to the new normalization is

$$(6.1) \quad x_j = \begin{cases} \log(z_{j+1} - z_j), & 1 \leq j \leq M - 2, \\ \frac{1}{2}[\log(z_M - z_{M-1}) + \log(z_{M+1} - z_{M+2})], & j = M - 1, \\ \log(z_{j+2} - z_{j+3}), & M \leq j \leq N - 3. \end{cases}$$

Note that there are only $N - 3$ independent variables, corresponding to the fact that now only $N - 3$ side length conditions are required to determine the shape of the closed polygon:

$$(6.2) \quad F_j = \begin{cases} \log \left| \frac{w_{j+1} - w_j}{w_{j+1}^* - w_j^*} \right|, & 1 \leq j \leq k - 2, \\ \log \left| \frac{w_{j+2} - w_{j+3}}{w_{j+2}^* - w_{j+3}^*} \right|, & k - 1 \leq j \leq N - 3. \end{cases}$$

Here w_k is the “omitted corner”—if $N - 1$ corners of the polygon and all of the angles are known, then the position of the remaining corner is determined and cannot be specified separately. The side between w_1 and w_N is fixed by the constants A and B , and the two sides that intersect at w_k do not enter into the parameter problem, so exactly $N - 3$ side lengths are sufficient to determine the shape of the polygon.

The best choice of w_k is problem-dependent, and an improper choice can make the system of nonlinear equations much more difficult to solve. In Fig. 8, for example, w_7 and w_8 would both be poor choices for w_k . Since the two sides that intersect at w_7 are collinear, it is not possible to determine the position of the corner by finding the

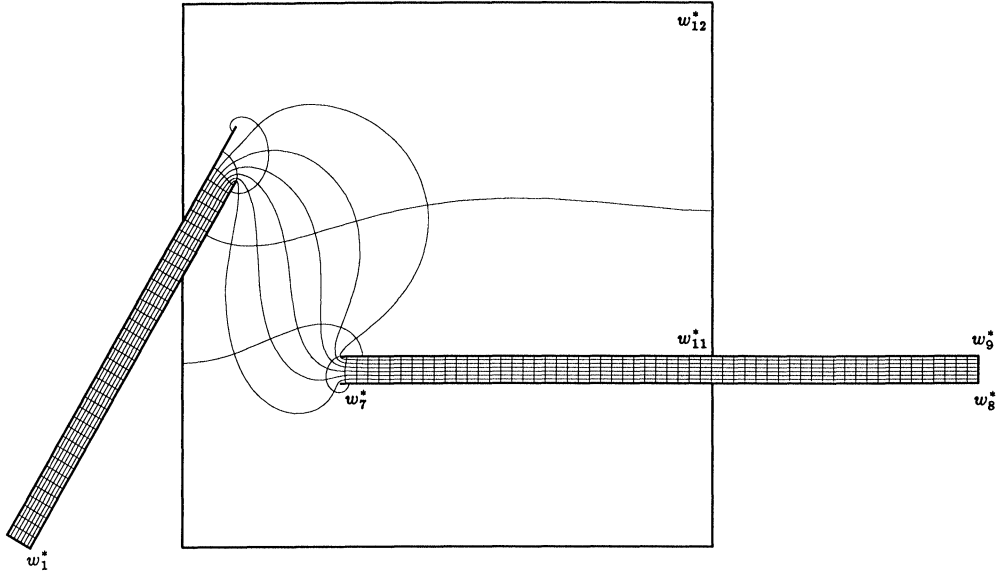


FIG. 8. Conformal map of a rectangle onto a distorted polygon ($\mu \approx 41.812465$).

intersection of the sides. To see why w_8 is bad, picture a slight distortion of this polygon in which the distance between w_{11} and w_{12} is increased and the horizontal tube is correspondingly narrowed. This narrowing increases the aspect ratio of the tube dramatically, so z_8 and z_9 would be far to the right of their correct positions. This will only affect the dependent variables to a small degree, though, if the distance between w_8 and w_9 is not included in (6.2). The system of nonlinear equations will therefore be poorly scaled, and the algorithm will probably take much longer to converge. A much better choice in this case would be w_{12} , which does not introduce any scaling problems. Several other choices would be equally good, and in fact it is sometimes helpful to change w_k in the middle of the solution process if the nonlinear equations algorithm is making slower progress.⁴

At present, our code leaves the choice of w_k up to the user, but we may be able to automate this in the future. Figure 9(a)–(b) shows two examples of regions for which no choice of w_k is very good: the only way to make these problems well scaled would be to devise a radically different set of dependent variables.⁵ Note that the self-intersecting nature of the first domain does not cause any difficulties; the problem results from the fact that changing almost any side length slightly can greatly alter the conformal modulus of the polygon.

7. Variations. The two problem formulations described in §§ 4 and 6 illustrate some of the choices that can be made with the strip transformation, but by no means do they exhaust the possibilities. With the channel mapping, for instance, it is not

⁴ The system of equations for the channel map can be altered in a similar manner, but the presence of the angle in (4.3) raises complications. One must be careful not to create a set of nonlinear equations with more than one solution.

⁵ It is still possible to calculate accurate conformal moduli for these polygons, however, even though the parameter problems are slow to converge. So that others may reproduce these examples if they wish, in the star the width of the strip is $1/20$ of the radius of the circumscribing circle, and in the spiral the width of the strip is exactly half the width of the complementary white space. The regions shown in Figs. 8 and 10(b) have corners exactly: $\{(-.2887, 0.), (.1, .6732), (0., .4999), (0., 0.), (1., 0.), (1., .2999), (.3, .3), (1.5, .3), (1.5, .35), (.3, .35), (1., .3501), (1., 1.), (0., 1.), (0., .6001), (.1, .7732), (-.3320, .025)\}$ and $\{(0., 8.), (1.8, 8.), (1.8, 0.), (13., 0.), (14., 0.), (14., 1.), (2., 1.), (2., 10.), (0., 10.)\}$, respectively.

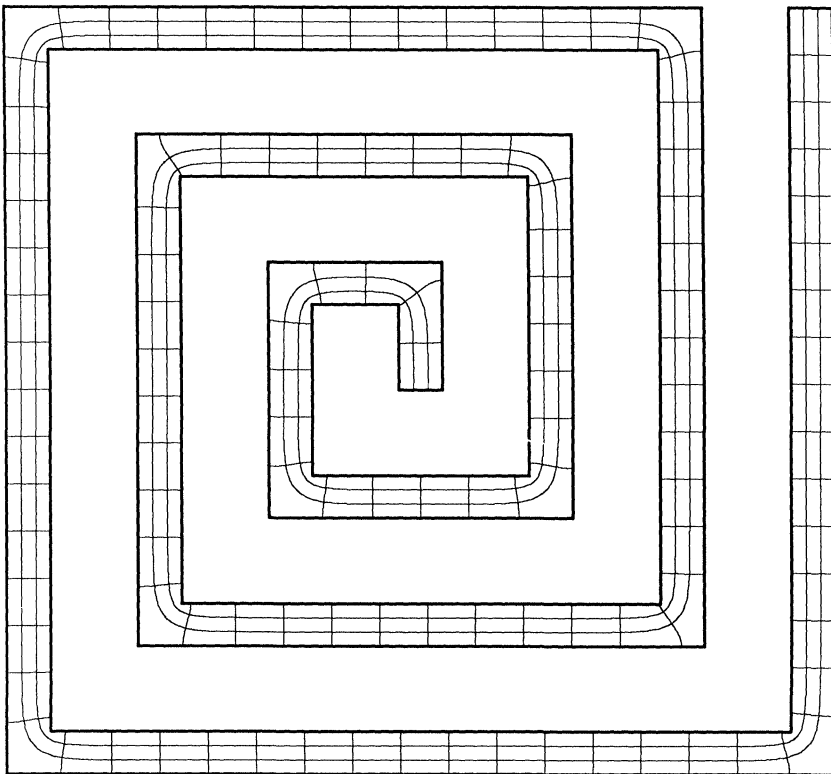
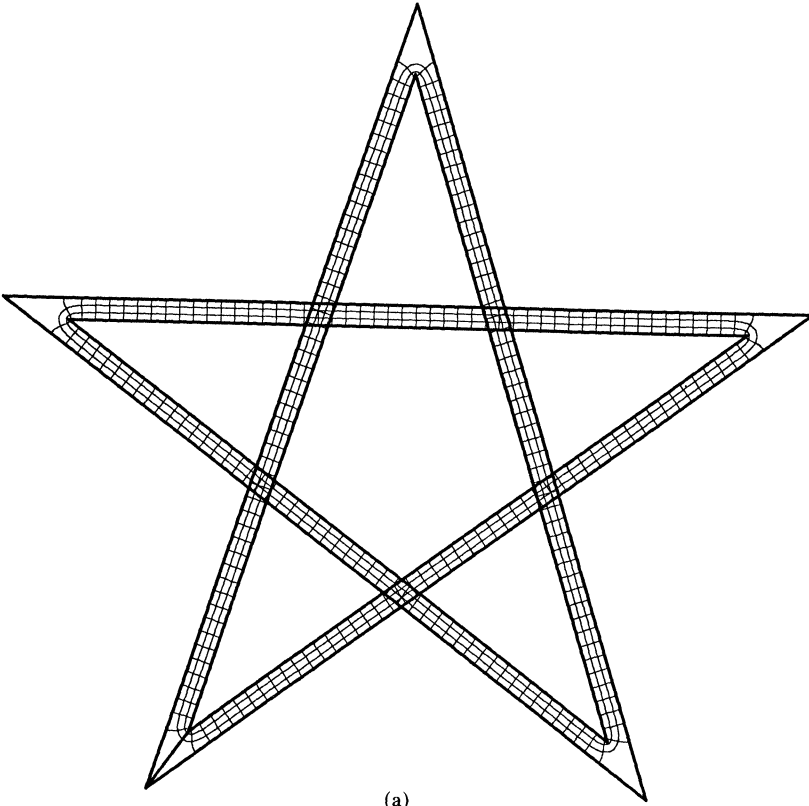


FIG. 9. (a) Conformal map of a rectangle onto a star ($\mu \approx 163.28151$). Note that both ends of the polygon meet at the lower-left corner. (b) Conformal map of a rectangle onto a finite spiral ($\mu \approx 132.70454$).

necessary for either of the divergence angles θ_- and θ_+ to be positive; the channel may be bounded. Figure 10(a) shows an example where both are negative; physically this could represent an electromagnetic problem with point charges or currents, or a fluids problem with a source and a sink. (This region has significant secondary crowding effects near the point of the barb, due to the extremely acute angle there. It is impossible to plot streamlines much closer to the point than those shown using the integration methods we have described. The other angles are wide enough to avoid this difficulty, though there is always some degradation of accuracy near an outward-pointing corner.)

With the rectangle mapping there is no reason why each end of the rectangle must map onto a single side of the polygon, and there are many possible ways to modify

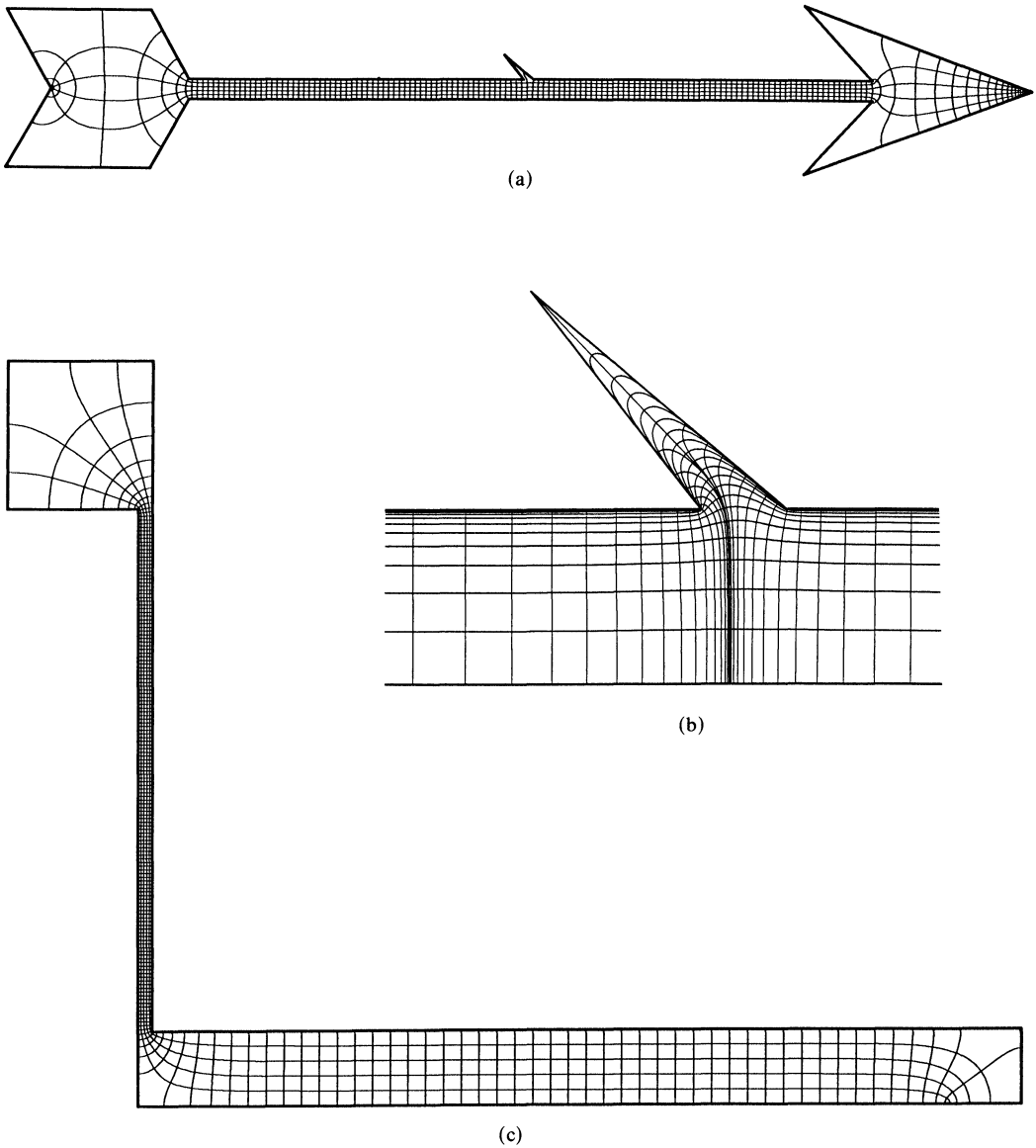


FIG. 10. (a) A channel map with converging ends; (b) enlargement of the barb in Fig. 10(a); (c) a rectangle map onto a polygonal conductor ($\mu \approx 49.436547$).

the given formulation to deal with unusual cases. In Fig. 10(c), for example, we have fixed w_{N-1}^* at i instead of w_N^* , and introduced an additional vertex w_4 with a turning angle of 0. Problems like this one could arise in integrated circuit design.

Other straightforward variations of the method described in this paper include vertices at infinity, the exterior map for a polygon, the map from a semi-infinite strip to a channel bounded at one end, and various generalized parameter problems as those described in [30] and [8].

Figure 11 shows a more extreme variation, an infinite logarithmic spiral. To permit our program to run to completion in a finite time, we truncated the infinite product in (3.5) by ignoring corners more than three turns away from the point of interest. This approach yields accurate results since the effect of each singularity decays exponentially along the strip. The parameter problem for this example is also quite simple, since the domain is self-similar; we omit the details. A similar formulation was used by Floryan [10] to map periodic channel configurations. The ideas involved in this example might possibly be extended to permit the mapping of more complicated fractal domains, which would have applications, for example, in the study of diffusion-limited aggregation.

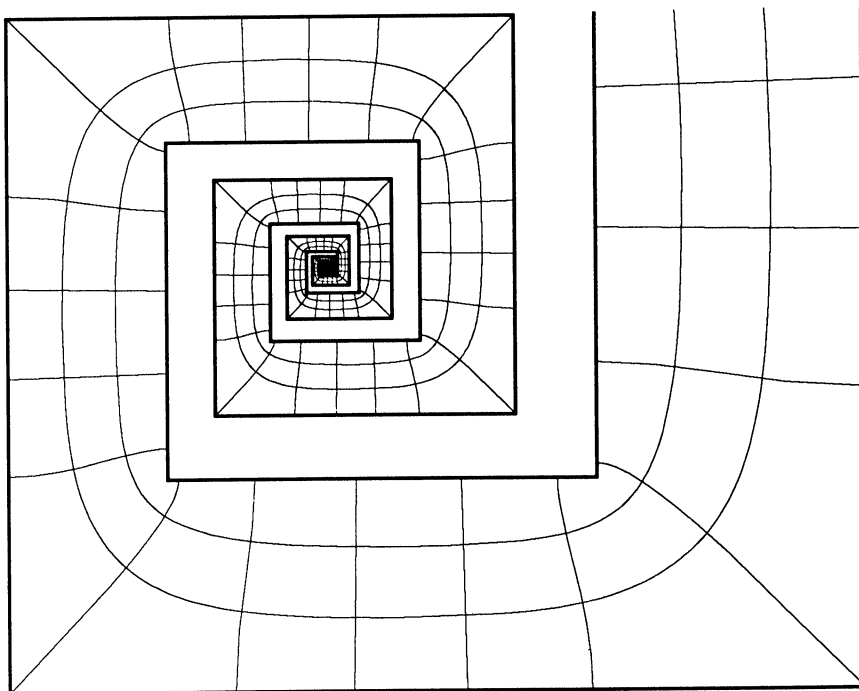


FIG. 11. *Conformal map onto an infinite spiral.*

Sridhar and Davis [3], [27], Floryan [9], and Hoekstra [19] have all described another variation of channel maps for approximating curved boundaries, based on formulas dating back at least to Woods [33]. Our implementation does not currently include this variation, but it would certainly be a valuable addition to any future software package for calculating Schwarz-Christoffel maps.

8. Conclusion. To summarize the central point of this paper: Conformal maps of highly elongated polygons should be based on a Schwarz-Christoffel formula for an

infinite strip, not a disk or a half plane. Many of the polygons that arise in applications are of this type—perhaps most.

The mathematics of the Schwarz–Christoffel formula for an infinite strip is not new. What is new here is, first, the proposal that such a formula could be used even when the polygon is bounded rather than an infinite channel, and second, an algorithm for numerical integration and solution of the parameter problem that can reliably and efficiently compute conformal maps to high accuracy (e.g., 8 or 12 digits, except in regions subject to secondary crowding) even for extremely elongated polygons (e.g., with aspect ratios in the hundreds or thousands). The elements of this algorithm are adapted from the SCPACK package for mapping the unit disk.

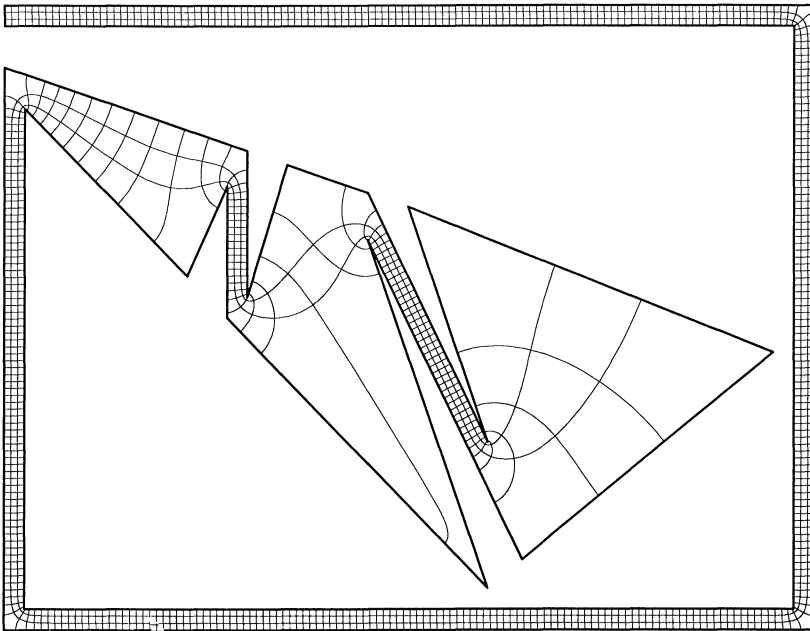


FIG. 12. A polygon with 23 sides ($\mu \approx 156.6241139$).

We conclude with a final example. The rather difficult 23-sided polygon of Fig. 12 was mapped from a rectangle, to roughly 10-digit precision, in about one hour on a Sun 3/50 with an MC68881 floating-point coprocessor. Most of this time was spent in solving the parameter problem, and since the final convergence is quite rapid, the time is nearly independent of the required accuracy. The same calculation on a supercomputer would require only a few seconds.

Appendix. Evaluation of elliptic functions. The use of the rectangle mapping described in §6 requires the efficient evaluation of the function $s(z) = (1/\pi) \log \operatorname{sn}(z|m)$ over a wide range of values of z and m . All of the formulas we use for these computations are well known and available in standard references, but since there are several different asymptotic regimes involved, it seems appropriate to give a brief summary of our methods here. For more information about any of the following material, see [1].

The parameter m of the elliptic function $\operatorname{sn}(z|m)$ decreases exponentially with $K'/2K$, the conformal modulus of the rectangle. For highly elongated regions, therefore,

m may be less than the underflow limit of many computers. First we will deal with the case where m is reasonably large; in our own program this means $m > 10^{-30}$.

To start with, the value of L is determined by the solution to the parameter problem for the strip transformation, so $m = e^{-2\pi L}$ is known immediately. K and K' are complete elliptic integrals with parameter m , and can be readily found by means of the arithmetic-geometric mean (AGM) method. To calculate K we first take

$$(A.1) \quad a_0 = 1, \quad b_0 = \sqrt{m_1}, \quad c_0 = \sqrt{m};$$

$m_1 = 1 - m$ is called the complementary parameter. The AGM iteration, defined by the formulas

$$(A.2) \quad a_i := \frac{1}{2}(a_{i-1} + b_{i-1}), \quad b_i := (a_{i-1}b_{i-1})^{1/2}, \quad c_i := \frac{1}{2}(a_{i-1} - b_{i-1}),$$

is then carried out until at the N th step c_N is negligible to the required accuracy. K is then equal to $\pi/2a_N$; to find K' the same procedure is followed with m and m_1 interchanged.

We need to evaluate $\text{sn}(z|m)$ at points inside the rectangle with corners $-K, K, K + iK', -K + iK'$. This function has a pole at iK' , but we avoid any difficulties there by using the identity

$$(A.3) \quad \text{sn}(z|m) = \frac{-1}{m^{1/2} \text{sn}(iK' - z|m)}$$

whenever $\text{Im}(z) > K'/2$. For $\text{Im}(z) \leq K'/2$ we can approximate $\text{sn}(z|m)$ by

$$(A.4) \quad \text{sn}(z|m) \sim \sin(z) - \frac{1}{4}m[z - \sin(z)\cos(z)]\cos(z)$$

when m is small enough; the relative accuracy of this formula is $O(m)$ for $\text{Im}(z) \leq K'/2$. If m is not sufficiently small we can reduce it by applying the descending Landen transformation as many times as necessary:

$$(A.5) \quad \mu = \left(\frac{1 - m_1^{1/2}}{1 + m_1^{1/2}} \right)^2,$$

$$(A.6) \quad v = \frac{z}{1 + \mu^{1/2}},$$

$$(A.7) \quad \text{sn}(z|m) = \frac{(1 + \mu^{1/2}) \text{sn}(v|\mu)}{1 + \mu^{1/2} \text{sn}^2(v|\mu)}.$$

The effect is to replace m and z by μ (not to be confused with the conformal modulus) and v , where $\mu \sim m^2/16$ and $v \sim z$. To avoid cancellation errors, (A.5) should be evaluated via a power series when m is less than about 10^{-3} .

When $L > 11$, i.e., $m < 10^{-30}$, we use a different set of asymptotic formulas to avoid possible underflow of m or overflow of $\text{sn}(z|m)$. K and K' are calculated via the approximations

$$(A.8) \quad K \sim \frac{\pi}{2} \quad \text{and} \quad K' \sim \pi L + \log 4,$$

which are accurate to $O(m)$. For $\text{Im}(z) \leq K'/2$ the approximation $\text{sn}(z|m) \sim \sin(z)$ has a relative accuracy of $O(m^{1/2})$, and $\log(\sin z)$ can be expanded to give

$$(A.9) \quad s(z) \sim \frac{1}{\pi} \left\{ -iz + \log \left[\frac{1}{2i} (e^{2iz} - 1) \right] \right\}.$$

When $\text{Im}(z) > K'/2$ the identity (A.3) leads to the similar formula

$$(A.10) \quad s(z) \sim L + i + \frac{1}{\pi} \left\{ iu - \log \left[\frac{1}{2i} (e^{2iu} - 1) \right] \right\},$$

where $u = iK' - z$.

By the methods described here we can evaluate $s(z) = (1/\pi) \log \text{sn}(z|m)$ to close to full precision (around 15 decimal places in our calculations), for all z in the fundamental rectangle, for a range of parameters roughly $e^{-2\pi/\varepsilon} \ll m < \frac{1}{2}$, that is, $O(1) \leq L \ll \varepsilon^{-1}$, where ε is the machine precision.

REFERENCES

- [1] M. ABRAMOWITZ AND I. STEGUN, EDs., *Handbook of Mathematical Functions*, National Bureau of Standards, Washington, D.C., 1964.
- [2] P. BJØRSTAD AND E. GROSSE, *Conformal mapping of circular arc polygons*, SIAM J. Sci. Statist. Comput., 8 (1987), pp. 19-32.
- [3] R. T. DAVIS, *Numerical methods for coordinate generation based on Schwarz-Christoffel transformations*, Proc. 4th Amer. Inst. Aero. Astro. Computational Fluid Dynamics Conference, Williamsburg, VA, 1979.
- [4] J. E. DENNIS JR. AND R. B. SCHNABEL, *Numerical Methods for Unconstrained Optimization and Nonlinear Equations*, Prentice-Hall, Englewood Cliffs, NJ, 1983.
- [5] F. DIAS, *On the use of the Schwarz-Christoffel transformation for the numerical solution of potential flow problems*, Ph.D. thesis, University of Wisconsin, Madison, WI, 1986.
- [6] J. J. DONGARRA AND E. GROSSE, *Distribution of mathematical software via electronic mail*, Commun. ACM, 30 (1987), pp. 403-407.
- [7] M. DUBINER, *Theoretical and numerical analysis of conformal mapping*, Ph.D. thesis, Department of Mathematics, Massachusetts Institute of Technology, Cambridge, MA, 1981.
- [8] A. R. ELCRAT AND L. N. TREFETHEN, *Classical free-streamline flow over a polygonal obstacle*, J. Comput. Appl. Math., 14 (1986), pp. 251-265.
- [9] J. M. FLORYAN, *Conformal-mapping-based coordinate generation method for channel flows*, J. Comput. Phys., 58 (1985), pp. 229-245.
- [10] ———, *Conformal-mapping-based coordinate generation method for flows in periodic configurations*, J. Comput. Phys., 62 (1986), pp. 221-247.
- [11] J. M. FLORYAN AND C. ZEMACH, *Schwarz-Christoffel mappings: A general approach*, J. Comput. Phys., 72 (1987), pp. 347-371.
- [12] ———, *Quadrature rules for singular integrals with application to Schwarz-Christoffel mappings*, J. Comput. Phys., 75 (1988), pp. 15-30.
- [13] G. E. FORSYTHE, M. A. MALCOLM, AND C. B. MOLER, *Computer Methods for Mathematical Computations*, Prentice-Hall, Englewood Cliffs, NJ, 1977.
- [14] D. GAIER, *Ermittlung des konformen Moduls von Vierecken mit Differenzenmethoden*, Numer. Math., 19 (1972), pp. 179-194.
- [15] A. F. GHONIEM AND Y. GAGNON, *Vortex simulation of laminar recirculating flow*, J. Comput. Phys., 68 (1987), pp. 346-377.
- [16] G. H. GOLUB AND J. H. WELSCH, *Calculation of Gaussian quadrature rules*, Math. Comp., 23 (1969), pp. 221-230.
- [17] L. GREENGARD, *Potential flow in channels*, SIAM J. Sci. Statist. Comput., submitted.
- [18] P. HENRICI, *Applied and Computational Complex Analysis*, Vol. 3, John Wiley, New York, 1986.
- [19] M. HOEKSTRA, *Coordinate generation in symmetrical interior, exterior or annular 2-D domains, using a generalized Schwarz-Christoffel transformation*, in Numerical Grid Generation in Computational Fluid Mechanics, J. Hauser and C. Taylor, eds., Pineridge Press, Swansea, United Kingdom, 1986.
- [20] L. V. KANTOROVICH AND V. I. KRYLOV, *Approximate Methods of Higher Analysis*, P. Noordhoff, Groningen, the Netherlands, 1958.
- [21] R. MENIKOFF AND C. ZEMACH, *Methods for numerical conformal mapping*, J. Comput. Phys., 36 (1980), pp. 366-410.
- [22] J. J. MORÉ, B. S. GARBOW, AND K. E. HILLSTROM, *User guide for MINPACK-1*, Argonne National Laboratory Report, ANL-80-74, Argonne, IL, 1980.

- [23] N. PAMAMICHAEL, C. A. KOKKINOS, AND M. K. WARBY, *Numerical techniques for conformal mapping onto a rectangle*, J. Comput. Appl. Math., 20 (1987), pp. 349–358.
- [24] R. PIESSENS, E. DE DONCKER-KAPENGA, C. W. ÜBERHUBER, AND D. K. KAHANER, *QUADPACK: A Subroutine Package for Automatic Integration*, Springer-Verlag, Berlin, New York, 1983.
- [25] M. J. D. POWELL, *A Fortran subroutine for solving systems of non-linear algebraic equations*, Tech. Report AERE-R. 5947, Harwell, England, 1968.
- [26] K. REPPE, *Berechnung von Magnetfeldern mit Hilfe der konformen Abbildung durch numerische Integration der Abbildungsfunktion von Schwarz-Christoffel*, Siemens Forsch. u. Entwickl. Ber., 8 (1979), pp. 190–195.
- [27] K. P. SRIDHAR AND R. T. DAVIS, *A Schwarz-Christoffel method for generating two-dimensional flow grids*, J. Fluids Eng., 107 (1985), pp. 330–337.
- [28] L. N. TREFETHEN, *Numerical computation of the Schwarz-Christoffel transformation*, SIAM J. Sci. Statist. Comput., 1 (1980), pp. 82–102.
- [29] ———, *SCPACK User's Guide*, Numerical Analysis Report 89-2, Department of Mathematics, Massachusetts Institute of Technology, Cambridge, MA, 1989.
- [30] ———, *Analysis and design of polygonal resistors by conformal mapping*, J. Appl. Math. Phys., 35 (1984), pp. 692–704.
- [31] ———, ED., *Numerical Conformal Mapping*, North-Holland, Amsterdam, 1986.
- [32] ———, *Schwarz-Christoffel mapping in the 1980's*, Numerical Analysis Report 89-1, Department of Mathematics, Massachusetts Institute of Technology, Cambridge, MA, 1989.
- [33] L. C. WOODS, *The Theory of Subsonic Plane Flow*, Cambridge University Press, United Kingdom, 1961.